metals

MDPI

*Review*

# Duplex and Superduplex Stainless Steels: Microstructure and Property Evolution by Surface Modification Processes

**Alisiya Biserova Tahchieva [1,*], Núria Llorca-Isern [1] and José-María Cabrera [2]**

[1] PROCOMAME, Departament de Ciència de Materials i Química Física, Facultat de Química, Universitat de Barcelona, 08028 Barcelona, Spain; nullorca@ub.edu

[2] PROCOMAME, Departament de Ciència dels Materials i Enginyeria Metal·lúrgica, EEBE, Universitat Politècnica de Catalunya 2, 08019 Barcelona, Spain; jose.maria.cabrera@upc.edu

* Correspondence: abiserova.tahchieva@ub.edu; Tel.: +34-934-039-621

Received: 7 February 2019; Accepted: 13 March 2019; Published: 19 March 2019


**Abstract:** The paper presents an overview of diffusion surface treatments, especially nitriding processes, applied to duplex and superduplex stainless steels in the last five years. Research has been done mainly to investigate different nitriding processes in order to optimize parameters for the most appropriate procedure. The scope has been to improve mechanical and wear resistance without prejudice to the corrosion properties of the duplex and superduplex stainless steels. Our investigation also aimed to understand the effect of the nitriding layer on the precipitation of secondary phases after any heating step.

**Keywords:** duplex stainless steels; superduplex stainless steels; nitriding; secondary phases; surface treatments

## 1. Duplex and Super Duplex Stainless Steels

Duplex stainless steels (DSSs) are stainless steels classified according to their composition and thermomechanical treatment. DSSs are characterized by their microstructure, which contains both delta ferrite and austenite phases with approximately equal volume fractions, and an unusual combination of mechanical strength, toughness, and corrosion resistance [1]. Because of their content of Cr, Mo, and N, these steels are particularly resistant to pitting corrosion and can be differentiated in terms of pitting resistance equivalent number (PREN), which is often defined as:

$$\text{PREN} = \%\text{Cr} + 3.3\ (\%\text{Mo}) + 16\ (\%\text{N}). \quad (1)$$

Typically, DSSs contain 17–30 wt% Cr and 3–13 wt% Ni [2], and according to Equation (1), the addition of chromium, molybdenum, and nitrogen raises the pitting corrosion resistance. PREN is useful for comparing and ranking the grades of duplex stainless steels, but it can rarely be useful as a prediction for a suitable application. Duplex stainless steels with a PREN higher than 40 are extremely resistant to pitting corrosion and are designated as super DSS (SDSS) [3].

Due to the promising corrosion properties, a high mechanical strength combined with a good toughness, SDSS are widely used in chemical tankers, in the petrochemical industry as well as in marine and nuclear power industries [4–6]. However, studies for new alloys with even higher strength than that of the DSSs and SDSSs have increased in the past few years with new demanding applications, especially in the oil and gas industry [7]. For these challenges, new high alloyed duplex stainless steels have been developed and are characterized by a PREN close to 50, termed as hyper duplex stainless steels (HDSS) [8,9].

With respect to applications, one of the main restrictions of duplex stainless steels has been the exposure to elevated temperatures. The unstable ferrite phase at higher temperatures leads to its decomposition and degradation of both mechanical and corrosion properties [3]. In the temperature range 250–500 °C, decomposition of ferrite and embrittlement may occur after long-term exposure, inducing a decrease in toughness. At higher temperatures, various types of precipitates may form in the range of 600–900 °C, leading to a reduction in corrosion resistance and/or reduction of toughness as well [5]. A variety of secondary phases, mostly undesirable, may form during isothermal aging or inappropriate heat treatments, essentially from the instability mentioned before [5]. The following phases have been observed and have been under investigation for a long time: σ phase [10–12], $Cr_2N$, CrN [13,14], secondary austenite, χ phase [14–16], R phase, π phase, $M_7C_3$, $M_{23}C_6$, and τ phase. A lot of literature can be found regarding their formation as well as conditions and properties influencing mostly the mechanical and corrosion resistance of duplex and super duplex stainless steels [5,17–20].

Despite the excellent mechanical strength and corrosion resistance of DSS and SDSS, they have limited applications in industries where high wear resistance together with corrosion resistance are required. Thus, another restriction can be found in the tribological applications. Fortunately, in the past years, exponential development in surface engineering has been done, and consequently, an important improvement in surface hardness and tribological properties is possible, even in unusual alloys.

## 2. Surface Modification Technologies

Diffusion surface treatments including nitriding, carburizing, or nitrocarburizing can be performed under a controlled gas atmosphere as well as under plasma conditions [21–23]. Nitriding can be applied to unalloyed steels and irons to produce a corrosion and wear-resistant nitride layer. In alloyed steels containing nitride-forming elements (Cr, Mn, Mo, V, W, Al, Ti) a deeper diffusion layer develops. Nitriding techniques are suitable for the enhancement of wear resistance, improving hardness up to 1400 HV. However, due to the high content of chromium, nitride layers tend to be formed as a result of the strong bonding energy between chromium and nitrogen. Thus, chromium nitride precipitation occurs, which decreases the corrosion resistance. The precipitation of the other phases already mentioned is also critical for the corrosion and/or mechanical properties. Nevertheless, a moderate formation of the sigma phase is tolerable and can imply an improvement in the wear resistance. Among the possible solutions to this problem, the development of an appropriate coating is critical. The goal is to produce layers of high hardness on the steel to improve tribological performance without degrading the corrosion resistance. Such coating can be achieved by accurate nitriding. Nitriding techniques can differ among others in the nitriding media and process parameters such as temperature, time, composition of the nitriding atmosphere, and pressure [24–26].

Nitriding processes of austenitic stainless steels (fcc phase) are the most studied for the enhancement of hardness and wear properties. Thermochemical surface engineering has been investigated as an effective path by alloying the surface with interstitial elements, such as C and N, at elevated temperatures via diffusion. The nitrogen inlet produces a supersaturated austenite phase, which enhances the surface tribology and corrosion resistances. [27,28]. This phase has been the object of extensive investigation. In the 1980s and 1990s, research demonstrated that the surface hardness was improved without loss of corrosion resistance by low temperature nitriding or carburizing [29–33], mainly because of the lack of Cr nitrides or carbides precipitated at temperatures below 500 °C [23]. Ichii et al. [34] studied the evolution of phase transformation that takes place during the process. The XRD pattern of low temperature plasma nitride austenitic stainless steel contained five extra peaks shifted to the lower diffraction angles relative to the corresponding γ peaks. As they were not listed in the ASTM (American Society for Testing and Materials) index, Ichii et al. denoted the term S-phase to describe the new phase. The term "expanded austenite" ($\gamma_N$) associated to this S-phase was used for the first time by Leyland et al. in 1993 [35]. S-phase, or expanded austenite, has received wide scientific interest and is considered as one of the most important issues in surface engineering research. During the last decade, several techniques to form S-phase in austenitic stainless steels have

been developed. It has been also demonstrated that this phase can be generated in Ni-Cr, Co-Cr, and Co-Cr-Mo alloys [36–39].

The expanded austenite phase ($\gamma_N$) evolved with the understanding of its crystallographic structure. It was described as a duplex layer consisting of a microstructure of fcc $\gamma'$ [(Fe, Cr, N)$_4$ N] [23] and austenite or a compound layer with a structure of $M_4N$ [*M* = (Fe, Cr, Ni, ... ] [34]. It distinguishes from $\gamma$ by the high N-content, its concentration in solid solution reaches up to 25–38% in $\gamma_N$ in comparison to the equilibrium solubility of <0.65 at % in austenitic AISI316 [23,29,40,41]. $\gamma_N$ is also characterized by lattice rotation processes in the expanded fcc structure, which cause anisotropic distortions in the normal surface direction [42,43]. A very interesting microstructural analysis concerning N content and the properties associated to S-phase was carried out by Dahm and Dearnley [44].

On the other hand, the nitrogen diffusion to ferritic $\alpha$ stainless steel (bcc crystal structure) leads to the formation of iron nitrides ($\varepsilon$-$Fe_{2\text{-}3}N$, $\gamma'$-$Fe_4N$) and nitrides such as CrN [45,46]. The nitrogen solubility in a ferrite structure increases with chromium content, but decreases its diffusivity and is mostly found along the grain boundaries instead of being homogenously distributed interstitially [47,48]. Hence, the main differences observed between austenite and ferrite structures regarding nitriding process are the result of the thermodynamic conditions, since both phases present different nitrogen diffusion rates.

Duplex stainless steel and super duplex stainless steels contain both austenite and ferrite phases. Eventually, expanded phases in austenite grains and nitride precipitates in ferrite grain boundaries are expected [49]. However, this cannot be a general rule because it depends on the processing conditions and the varied compositions in different alloys [28].

In the last five years, some scientific publications have been done with the objective of understanding the morphology, structure, and composition of nitride layers in nitrided duplex stainless steels. The corrosion response by varying process parameters, or trying to combine different methods of nitriding and/or nitrocarburizing, has been mainly examined. The objective was to study the nature of the nitrogen-rich layer. One of the most important variables during the process is the temperature. Thus, low and high nitriding temperature processes can be differentiated among the works. For instance, several authors have demonstrated the formation of expanded austenite in DSS by nitriding at low temperature, assuring good corrosion resistance and improvement in hardness. This is due to the fact that chromium nitride formation is avoided at lower temperatures. Paijan et al. [26] revealed this fact by analyzing DSS samples after nitriding in a tubular furnace in the temperature range of 400 to 500 °C, holding for 6 h. Several researchers [26,50,51] found that above 500 °C chromium nitride precipitates are formed in the nitrogen-enriched layer, significantly reducing the corrosion resistance. It was also observed by Blawert et al. [52] and Larisch et al. [46] that after low temperature plasma nitriding of duplex stainless steel, transformation of ferrite into the expanded austenite phase after nitrogen incorporation took place. Bielawski et al. [24] and Chiu et al. [53] reported the generation of expanded ferrite ($\alpha_N$) and expanded austenite ($\gamma_N$) in both ferrite and austenite phases, respectively. Pinedo et al. [49] also explained the low-temperature plasma nitriding of duplex stainless steels carried out at 400 °C, which led to the formation of expanded austenite on the austenite stringers and expanded ferrite on the ferrite stringers of the microstructure. Moreover, some deformation bands were detected inside the expanded ferrite, which were assigned to compressive residual stresses, without chromium or iron nitride precipitation. On the contrary, in a more recent paper by Tschiptschin et al. [54] it was found that iron nitride ($\varepsilon$-$Fe_3N$) needles with a particular orientation relationship precipitate coherently inside the expanded ferrite regions of the nitride layer, increasing the hardness considerably. Similar $\varepsilon$-$Fe_3N$ needles were precipitated from nitrogen-saturated ferrite grains in a lean duplex stainless steel, as determined by Li et al. [55]. Both reports revealed by TEM that the S-phase could not be formed on lean duplex stainless steel by low-temperature plasma nitriding. Tschiptschin et al. [54] also revealed a duplex thermochemical diffusion treatment consisting of two steps, one gas nitriding conducted at high temperature and a final plasma nitriding at low temperature (HTGN + LTPN). UNS

S31803 duplex stainless steel was the alloy selected by these researchers, and they found an almost 4 µm-thick nitrogen-rich expanded austenite layer 1227 ± 78 HV00.1 formed on top of a high nitrogen austenitic layer of 330 HV hardness. This experiment ensured a more homogenous microstructure and gentler hardness gradients, with suitable properties for wear-bearing applications. Similar duplex thermochemical treatments were previously experimented by Mesa et al. in order to improve the cavitation resistance of the same duplex stainless steel [56].

Plasma nitrocarburizing influences the corrosion behavior in a similar way as plasma nitriding. The formation of a larger amount of CrN in the alloy leads to a poor corrosion resistance at temperatures between 450 and 500 °C. It was found by Alphonsa et al. [50] that treatments at 350 and 400 °C are beneficial, but 450 and 500 °C treatments are better suited to duplex stainless steels for applications requiring a combination of both high hardness (1010 HV0.01) and corrosion resistance, for which a better corrosion resistance maintaining high hardness values compared to the bare duplex stainless steel is observed.

Concerning the morphology of the layer formed after nitriding, some authors reported that the thickness of the layer is a function of the temperature. It was observed that the thickness over the two phases (austenite and ferrite) is different in the case of plasma nitride specimens, whereas such a difference was not found in the plasma nitrocarburized samples. However, it was also described that treatments above 500 °C lead to similar thicknesses over both phases [57].

The reason for the difference in nitrogen diffusion into the austenite and ferrite phases was discussed by Pinedo et al. [49] and Bobadilla and Tschiptschin [57]. Diffusion of nitrogen not only occurs in the volume of the substrate but also through the grain boundaries. The lateral flow of nitrogen tends to move from ferrite to the austenite in order to reach equilibrium.

Some authors studied the plasma variables (such as frequency, pulse width, and voltage) with the surface modification in order to understand nitriding plasma-based ion implantation [28]. Li et al. [55] suggested an optimized plasma nitriding process as the best treatment for lean duplex stainless steel for only 10 h at 450 °C and at 420 °C for dry-wear and corrosion-wear applications, respectively.

Most of the reported research mainly investigated the surface layer structure, morphology, hardness, corrosion, and mechanical resistance as well as tribological and tribocorrosion properties as a function of the type of nitriding processes mostly under low temperature procedures. Hence, our research aimed to study the plasma nitriding process applied to duplex stainless steel (S32205) and super duplex stainless steel (S32750) at high temperature, 520 °C, during a short nitriding time (10 h).

All samples were previously annealed to 1080 °C for 30 min and immediately quenched with water in order to homogenize the structure before performing the nitriding process. Characterization of the microstructure of the formed layers and their potential to precipitate secondary phases when a heat treatment is carried out on nitride steels is reported. Table 1 summarizes the chemical composition of both DSS and SDSS.

**Table 1.** Chemical composition of duplex and super duplex stainless steels.

| **Sample Identification** | **Chemical Composition wt %** | | | | | | | | | |
|---|---|---|---|---|---|---|---|---|---|---|
| UNS | C | Si | Mn | P | S | Cr | Ni | Mo | N | Cu |
| S32205 | 0.015 | 0.4 | 1.5 | 0.018 | 0.001 | 22.49 | 5.77 | 3.21 | 0.184 | 0.18 |
| S32750 | 0.018 | 0.26 | 0.84 | 0.019 | 0.001 | 25.08 | 6.880 | 3.82 | 0.294 | 0.17 |

Layer morphology of treated samples under the same conditions is shown in Figure 1. The layer structure appears with the outer zone enriched in nitrogen (Figure 1a,c,e). A line scan of some diffusion elements confirmed the nitride layer formation and the excellent continuous interphase within the substrate.

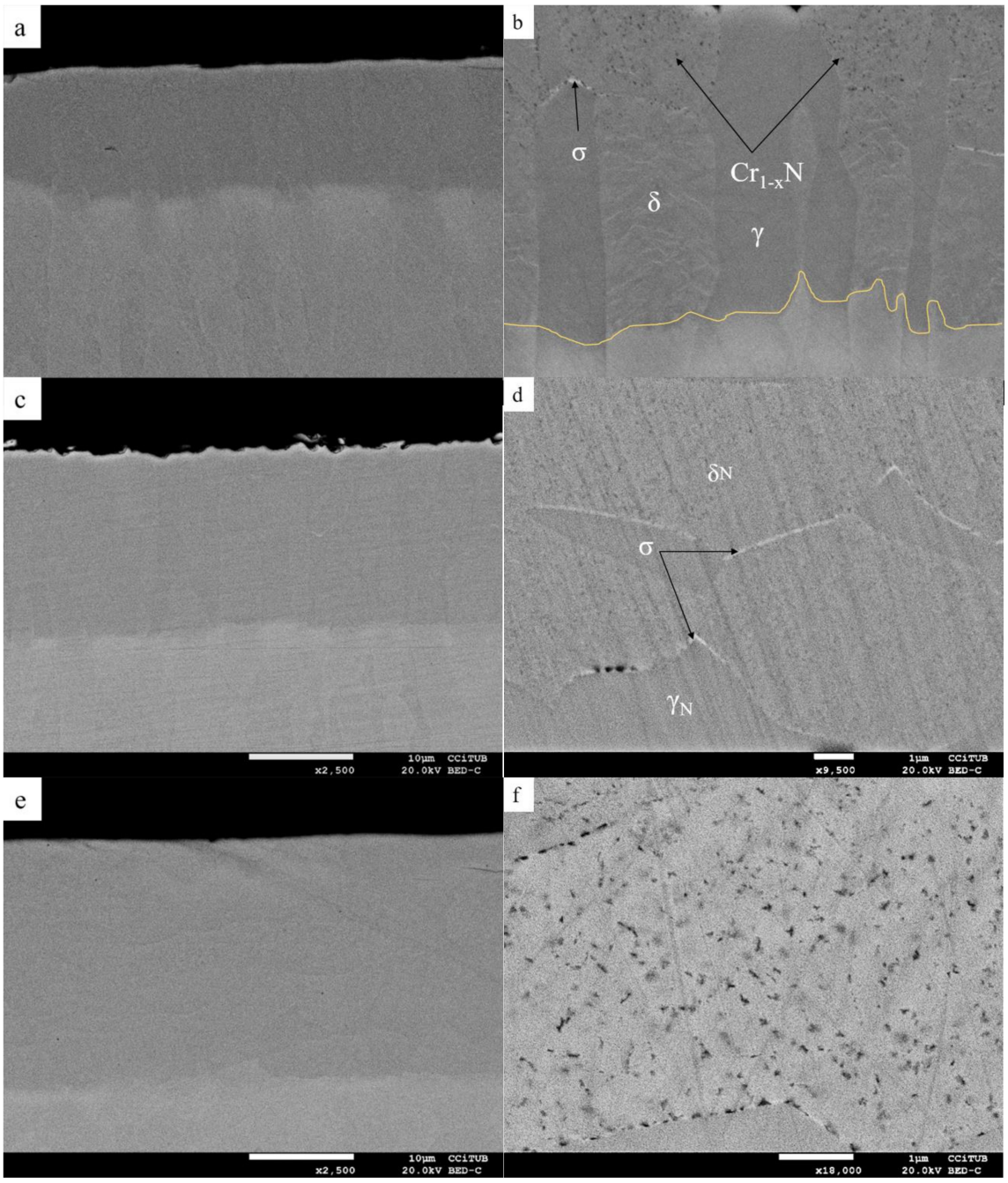


**Figure 1.** Backscattered electron (BSE) micrographs of super duplex stainless steel (SDSS) and duplex stainless steel (DSS) specimens after 10 h plasma nitriding at 520 °C. (**a**) Cross-section nitride layer of the SDSS tube. (**b**) Details of the nitride layer indicating the austenite (γ) and ferrite (δ) phases, as well as the sigma phase and chromium nitrides. (**c**) Cross-section of the nitride layer of the SDSS plate. (**d**) Higher magnification of the nitride layer in (**c**) showing expanded austenite $\gamma_N$ and expanded ferrite $\delta_N$ phases, as well as sigma phase in the boundaries. (**e**) Longitudinal section of the nitride layer of the DSS plate, and (**f**) higher magnification of the nitride layer (expanded ferrite $\delta_N$) on the DSS plate showing the distribution of chromium nitrides inside.

Backscattered electron (BSE) micrographs at higher magnification (Figure 1b,d,f) show the microstructure of samples extracted from the SDSS tube, SDSS plate, and DSS plate, respectively. Presence of a brighter phase at the grain boundaries of the expanded austenite and expanded ferrite phases is detected. This phase is associated with the sigma precipitate characteristic of duplex stainless steels after thermal treatments in the range of 600 to 850 °C. This phase was identified through the energy-dispersive X-ray spectroscopy (EDS) microanalyses showing a higher content of Mo than that of the ferrite phase. Precipitates of chromium nitrides (black dots) are also present and can be seen in Figure 1b as expected after nitriding at a temperature of 520 °C. These chromium nitride precipitates are apparently distributed only in the expanded austenite. Figure 1c,d shows the microstructure of SDSS samples extracted from the SDSS plate. Figure 1d shows the sigma precipitation linking the expanded austenite phase within the expanded ferrite phase. Chromium nitrides are also present inside both phases. The composition of the different phases was determined using a JEOL (Peabody, MA, USA) J-7100 field emission scanning electron microscope (FE-SEM) with an energy-dispersive X-ray spectroscopy system (EDS) INCA PentaFETx3 detector. In addition, a JEOL JXA-8230 microprobe (with five WDS spectrometers) allowed us to obtain a higher chemical composition accuracy. Different chemical compositions (such as differences in Mo, Cr) led to identify each phase.

A certain discordance was found between the literature and the present results, as the nitride layer showed an irregular thickness at the same temperature. Furthermore, the nitriding-substrate interface on austenite and ferrite phases is not regular (Figure 1b). It was predicted that for duplex stainless steel, a homogenous interphase and an almost equal thickness of nitride layer on austenite and ferrite phases of the substrate should be found above 500 °C [42]; however, SDSS does not follow this trend.

On the other hand, a Mo-enriched phase was not detected in the samples extracted from the DSS plate. This was probably due to the chemical composition of the alloy, as DSS had almost 0.5%wt less Mo than SDSS. Instead, DSS nitride layer accommodated more black spots, identified as nitrides. These nitrides are mainly found in the outer part of the nitrided steel layer and help raise the hardness of the nitrided steels (Figure 1f).

Hardness of the nitride layer was measured in order to check the improvement of the resistance strength obtained at a higher temperature of the plasma nitriding process. Minimum and maximum values of $HV_{0.3}$ and medium thickness with a standard deviation of the nitride layers are summarized in Table 2.

**Table 2.** Sample identification, $HV_{0.3}$ hardness (maximum and minimum range values), and medium thickness of the nitride layers.

| Material | $HV_{0.3}$ | Thickness Layer |
|---|---|---|
| Super Duplex S32750 tube | 1263 ÷ 1393 | 13.7 ± 0.0006 µm |
| Super Duplex S32750 plate | 1379 ÷ 1402 | 16.5 ± 0.0004 µm |
| Duplex S32205 plate | 1263 ÷ 1329 | 23.5 ± 0.0003 µm |

After the plasma nitriding process, thermal treatment at 830 °C for up to 3 min was carried out for the superduplex stainless steels. This treatment was selected in order to compare the precipitation of secondary phases before and after nitriding and the influence of a large concentration of nitrogen in that precipitation [58,59]. As observed in the images from backscattered electron microscopy (BSE) of SDSS plate cross-section (Figure 2a,b), precipitates of chromium nitride are identified inside the expanded ferrite phase. The sigma phase can also be seen in the ferrite–austenite grain boundaries, and inside the ferrite as well. The SDSS tube sample also shows the sigma phase precipitates. Less detectable is the presence of chromium nitrides, as can be observed in Figure 2c,d.

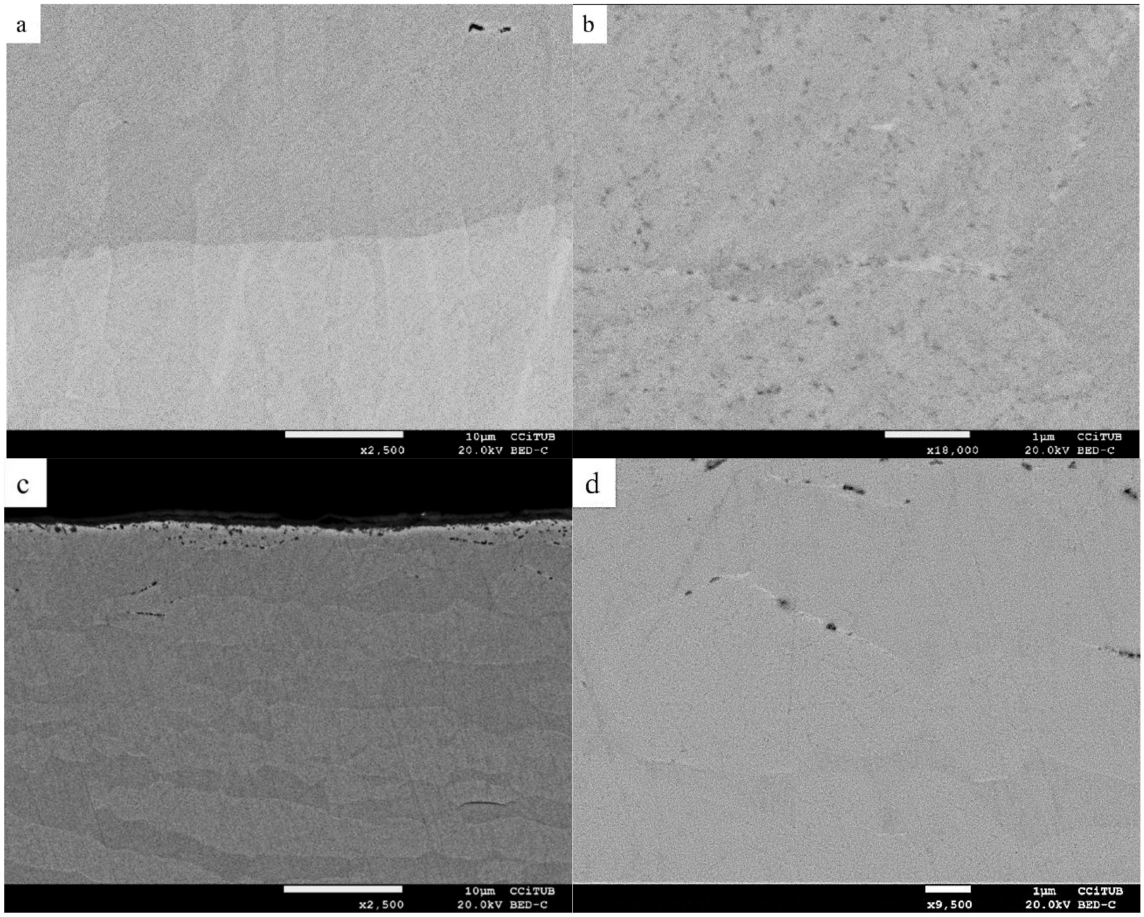


**Figure 2.** BSE micrographs of the SDSS plate and the SDSS tube samples after 10 h plasma nitriding at 520 °C and post heat treatment at 830 °C for up to 3 min. (**a**) Cross-section of the SDSS plate sample. (**b**) Higher magnification of (**a**). (**c**) Longitudinal section of the SDSS tube after 10 h, and (**d**) higher magnification of (**c**).

In light of the results, it can be observed that the thickness of the nitride layer formed at the same processing conditions was mainly influenced by the composition of the stainless steel. For instance, the DSS sample showed almost double the thickness of the SDSS samples. Nevertheless, both SDSS samples eventually presented higher hardness values because of the higher amount of chromium nitrides, which enhanced the hardness of the outer surface. Due to the high amount of nitrogen and chromium in SDSS compared with that of DSS, chromium nitrides were consequently formed in higher amounts. Another fact observed was that the microstructure resulting from the forming process was somehow influencing the diffusion through the steel. In this sense, rolled samples were previously annealed at 1080 °C for 30 min in order to homogenize them before performing the nitriding process, hence, only the formed microstructure remained before nitriding. The plate layer thickness was around 20% thicker than the tube layer thickness with the same processing conditions.

Secondary phases, mostly the sigma phase, were already formed within the nitriding process before any heat treatment was applied to the SDSS samples. Such behavior could not only be due to the temperature, but it can be regarded as high nitrogen ferrite and austenite help to induce its formation, even at temperatures as low as 520 °C. The nucleation and growth kinetics could be influenced by the previous forming process history of the specimen related to the texture and anisotropy developed in each case, as in the SDSS plate and the SDSS tube. Moreover, chromium nitrides act as a favorable site for the nucleation of the σ-phase.

However, heating the sample after nitriding sigma phase formation was clearly enhanced; the latter occurred mostly in the SDSS tube, as it was detected not only at the phase boundaries

(Figure 1b,d), but also in the austenite phase (Figure 2b). Surprisingly, the SDSS plate prepared longitudinally (Figure 2c,d) did not show the sigma phase inside the austenite phase. This again confirms the importance of the microstructure facing nitrogen diffusion: the diffusion path involving grain boundaries (favored by cross-sections facing the outer surface) will enhance nitrogen diffusion and, consequently, the induced formation of secondary phases. On the contrary, a longitudinal microstructure will limit the amount of nitrogen able to diffuse through austenite or ferrite phases.

## 3. Conclusion

Surface property enhancement of duplex stainless steels has been observed and supports the idea of an increasing demand on nitriding in order to enhance wear resistance. Plasma nitriding at 520 °C on duplex and superduplex stainless steels (UNS S32205 and S32750, respectively) has been carried out, and the characterization of the nitride layer formed has been studied. This layer is dense and well-formed and follows the microstructure of the steel. One of the main conclusions found is that layer thickness is dependent on the composition of the steel, hence, duplex and superduplex stainless steels show different thicknesses (~20%). Furthermore, nitrogen diffuses more intensively in ferrite, enhancing the formation of secondary phase precipitation (mainly sigma-phase) and its distribution along grain boundaries. Another interesting conclusion is that the oriented microstructure of ferrite and austenite from previous forming processes would influence the diffusion path of nitrogen. In this sense, plate samples showed a thicker nitriding layer than tube ones.

**Author Contributions:** All authors contributed to the conceptualization of the research, A.B.T., N.L.-I., and J.-M.C.; methodology of the review was created by A.B.T.; formal analyses were done by A.B.T., N.L.-I., and J.-M.C.; investigation was done by A.B.T.; resources were provided by all three authors, A.B.T., N.L.-I., and J.-M.C.; writing—original draft preparation was contributed by A.B.T.; writing—review and editing were done by A.B.T., N.L.-I., and J.-M.C.; supervision was carried out by all the authors, A.B.T., N.L.-I., and J.-M.C.

**Funding:** This research received no external funding.

**Acknowledgments:** The authors would like to thank S.A. Metalografica for the plasma nitriding process.

**Conflicts of Interest:** The authors declare no conflict of interest.

## References

1. Alvarez-Armas, I.; Degallaix-Moreuil, S. *Duplex Stainless Steels*; John Wiley and Sons: Hoboken, NJ, USA, 2009.
2. Lo, K.H.; Kwok, C.T.; Chan, W.K.; Kuan, H.C.; Lai, K.K.; Wang, K.Y. Duplex Stainless Steels. In *Encyclopedia of Iron, Steel, and Their Alloys*; CRC Press: Boca Raton, FL, USA, 2016; pp. 1150–1160.
3. Nilsson, J.O.; Wilson, A. Influence of isothermal phase transformations on toughness and pitting corrosion of super duplex stainless steel SAF 2507. *Mater. Sci. Technol.* **1993**, *9*, 545–554. [CrossRef]
4. Gunn, R. *Duplex Stainless Steels: Microstructure, Properties and Applications*; Woodhead Publishing: Cambridge, UK, 1997.
5. Nilsson, J.O. Super duplex stainless steels. *Mater. Sci. Technol.* **1992**, *8*, 685–700. [CrossRef]
6. Solomon, H.D.; Devine, T.M., Jr. *Duplex Stainless Steels—A Tale of Two Phases*; American Society for Metals: Metals Park, OH, USA, 1982; pp. 693–656.
7. Kangas, P.; Chai, G. Use of advanced austenitic and duplex stainless steels for applications in Oil & Gas and Process industry. *Century Stainl. Steels* **2013**, *794*, 645–669.
8. Chail, G.; Kangas, P. Super and hyper duplex stainless steels: Structures, properties and applications. *Procedia Struct. Integr.* **2016**, *2*, 1755–1762. [CrossRef]
9. Salvio, F.; da Silva, B.R.S. On the Role of HISC on Super and Hyper Duplex Stainless Steel Tubes. In Proceedings of the Offshore Technology Conference, Rio de Janeiro, Brazil, 29–31 October 2013.
10. Wan, J.; Ruan, H.; Wang, J.; Shi, S. The Kinetic diagram of sigma phase and its precipitation hardening effect on 15Cr-2Ni duplex stainless steel. *Mater. Sci. Eng. A* **2017**, *711*, 571–578. [CrossRef]
11. Atamert, S.; King, J.E. Sigma-phase formation and its prevention in duplex stainless steels. *J. Mater. Sci. Lett.* **1993**, *12*, 1144–1147. [CrossRef]

12. Chen, T.H.; Weng, K.L.; Yang, J.R. The effect of high-temperature exposure on the microstructural stability and toughness property in a 2205 duplex stainless steel. *Mater. Sci. Eng. A* **2002**, *338*, 259–270. [CrossRef]
13. Magnabosco, R.; Santos, D.C.d. Intermetallic Phases Formation During Short Aging between 850 °C and 950 °C of a Superduplex Stainless Steel. *J. Mater. Res. Technol.* **2012**, *26*. [CrossRef]
14. He, Y.-L.; Zhu, N.-Q.; Lu, X.-G.; Li, L. Experimental and computational study on microstructural evolution in 2205 duplex stainless steel during high temperature aging. *Mater. Sci. Eng. A* **2010**, *528*, 721–729. [CrossRef]
15. Escriba, D.M.; Materna-Morris, E.; Plaut, R.L.; Padilha, A.F. Chi-phase precipitation in a duplex stainless steel. *Mater. Charact.* **2009**, *60*, 1214–1219. [CrossRef]
16. Pohl, M.; Storz, O.; Glogowski, T. Effect of intermetallic precipitations on the properties of duplex stainless steel. *Mater. Charact.* **2006**, *58*, 65–71. [CrossRef]
17. Sieurin, H.; Sandström, R. Sigma phase precipitation in duplex stainless steel 2205. *Mater. Sci. Eng. A* **2007**, *444*, 271–276. [CrossRef]
18. Nilsson, J.O.; Liu, P. Aging at 400–600 °C of submerged arc welds of 22Cr–3Mo–8Ni duplex stainless steel and its effect on toughness and microstructure. *Mater. Sci. Technol.* **1991**, *7*, 853–862. [CrossRef]
19. Kim, Y.J.; Chumbley, L.S.; Gleeson, B. Determination of isothermal transformation diagrams for sigma-phase formation in cast duplex stainless steels CD3MN and CD3MWCuN. *Metall. Mater. Trans. A* **2004**, *35*, 3377–3386. [CrossRef]
20. Nilsson, J.O.; Karlsson, L.; Andersson, J.O. Secondary austenite for mation and its relation to pitting corrosion in duplex stainless steel weld metal. *Mater. Sci. Technol.* **1995**, *11*, 276–283. [CrossRef]
21. Kuwahara, H.; Matsuoka, H.; Takada, J.; Kikuchi, S.; Tomii, Y.; Tamura, I. Plasma nitriding of Fe-18Cr-9Ni in the range of 723?823 K. *Oxid. Met.* **1991**, *36*, 143–156. [CrossRef]
22. Flis, J.; Mańkowski, J.; Roliński, E. Corrosion Behaviour of Stainless Steels Aner Plasma and Ammonia Nitriding. *Surf. Eng.* **1989**, *5*, 151–157. [CrossRef]
23. Zhang, Z.L.; Bell, T. Structure and Corrosion resistance of plasma nitrided Stainless Steel. *Surf. Eng.* **1985**, *1*, 131–136. [CrossRef]
24. Bielawski, J.; Baranowska, J. Formation of nitrided layers on duplex steel—influence of multiphase substrate. *Surf. Eng.* **2010**, *26*, 299–304. [CrossRef]
25. Jasinski, J.J.; Fraczek, T.; Kurpaska, L.; Lubas, M.; Sitarz, M. Investigation of nitrogen transport in active screen plasma nitriding processes—Uphill diffusion effect. *J. Mol. Struct.* **2018**, *1164*, 37–44. [CrossRef]
26. Paijan, L.H.; Berhan, M.N.; Adenan, M.S.; Yusof, N.F.M.; Haruman, E. Structural Development of Expanded Austenite on Duplex Stainless Steel by Low Temperature Thermochemical Nitriding Process. *Adv. Mater. Res.* **2012**, *576*, 260–263. [CrossRef]
27. Dong, H. S-phase surface engineering of Fe–Cr, Co–Cr and Ni–Cr alloys. *Int. Mater. Rev.* **2010**, *55*, 65–98. [CrossRef]
28. De Oliveira, W.R.; Kurelo, B.C.E.S.; Ditzel, D.G.; Serbena, F.C.; Foerster, C.E.; de Souza, G.B. On the S-phase formation and the balanced plasma nitriding of austenitic-ferritic super duplex stainless steel. *Appl. Surf. Sci.* **2018**, *434*, 1161–1174. [CrossRef]
29. Sun, Y.; Li, X.; Bell, T. Structural characteristics of low temperature plasma carburised austenitic stainless steel. *Mater. Sci. Technol.* **1999**, *15*, 1171–1178. [CrossRef]
30. Mingolo, N.; Tschiptschin, A.P.; Pinedo, C.E. On the formation of expanded austenite during plasma nitriding of an AISI 316L austenitic stainless steel. *Surf. Coat. Technol.* **2006**, *201*, 4215–4218. [CrossRef]
31. Borgioli, F.; Fossati, A.; Galvanetto, E.; Bacci, T. Glow-discharge nitriding of AISI 316L austenitic stainless steel: Influence of treatment temperature. *Surf. Coat. Technol.* **2005**, *200*, 2474–2480. [CrossRef]
32. Fewell, M.P.; Mitchell, D.R.G.; Priest, J.M.; Short, K.T.; Collins, G.A. The nature of expanded austenite. *Surf. Coat. Technol.* **2000**, *131*, 300–306. [CrossRef]
33. Blawert, C.; Kalvelage, H.; Mordike, B.L.; Collins, G.A.; Short, K.T.; Jiraskova, Y.; Schneeweiss, O. Nitrogen and carbon expanded austenite. *Surf. Coat. Technol.* **2001**, *136*, 181–187. [CrossRef]
34. Ichii, T.; Fujimura, K.; Takase, K. Structure of the ion-nitrided layer of 18-8 stainless steel. *Tech. Rep. Kansai Univ.* **1986**, *27*, 134–144.
35. Leylanda, A.; Lewis, D.B.; Stevenson, P.R.; Matthewsa, A. Low temperature plasma diffusion treatment of stainless steels for improved wear resistance. *Surf. Coat. Technol.* **1993**, *62*, 608–617. [CrossRef]
36. Makishi, T.; Nakata, K. Surface Hardening of Nickel Alloys by Means of Plasma Nitriding. *Metall. Mater. Trans. A Phys. Metall. Mater. Sci.* **2004**, *35*, 227–238. [CrossRef]

37. Williamson, D.L.; Davis, J.A.; Wilbur, P.J. Effect of austenitic stainless steel composition on low-energy, high-flux, nitrogen ion beam processing. *Surf. Coat. Technol.* **1998**, *104*, 178–184. [CrossRef]
38. Li, X.Y.; Habibi, N.; Bell, T.; Dong, H. Microstructural characterisation of a plasma carburised low carbon Co–Cr alloy. *Surf. Eng.* **2007**, *23*, 45–51. [CrossRef]
39. Liu, R.; Li, X.; Hu, X.; Dong, H. Surface & Coatings Technology Surface modi fi cation of a medical grade Co–Cr–Mo alloy by low-temperature plasma surface alloying with nitrogen and carbon. *Surf. Coat. Technol.* **2013**, *232*, 906–911.
40. Williamson, D.L.; Wei, R.; Wilbur, P.J. Metastable phase formation and enhanced diffusion in f. c. c. alloys under high dose, high flux nitrogen implantation at high and low ion energies. *Surf. Coat. Technol.* **1994**, *65*, 15–23. [CrossRef]
41. Foerster, C.E.; Souza, J.F.P.; Silva, C.A.; Ueda, M.; Kuromoto, N.K.; Serbena, F.C.; Silva, S.L.R.; Lepienski, C.M. Effect of cathodic hydrogenation on the mechanical properties of AISI 304 stainless steel nitrided by ion implantation, glow discharge and plasma immersion ion implantation. *Nucl. Instrum. Methods Phys. Res. Sect. B Beam Interact. Mater. Atoms* **2007**, *257*, 727–731. [CrossRef]
42. Manova, D.; Mändl, S.; Neumann, H.; Rauschenbach, B. Formation of metastable diffusion layers in Cr-containing iron, cobalt and nickel alloys after nitrogen insertion. *Surf. Coat. Technol.* **2017**, *312*, 81–90. [CrossRef]
43. Stinville, J.C.; Villechaise, P.; Templier, C.; Rivière, J.P.; Drouet, M. Lattice rotation induced by plasma nitriding in a 316L polycrystalline stainless steel. *Acta Mater.* **2010**, *58*, 2814–2821. [CrossRef]
44. Dearnley, P.; Dahm, K.L.; Dearnley, P.A. On the Nature, Properties and Wear Response of S-phase (nitrogen-alloyed Stainless Steel) Coatings on Aisi 316l. *J. Mater. Des. Appl.* **2000**, *21*, 181–198.
45. Blawert, C.; Mordike, B.L.; Rensch, U.; Schreiber, G.; Oettel, H. Nitriding Response of Chromium Containing Ferritic Steels on Plasma Immersion Ion Implantation at Elevated Temperature. *Surf. Eng.* **2002**, *18*, 249–254. [CrossRef]
46. Larisch, B.; Brusky, U.; Spies, H.-J. Plasma nitriding of stainless steels at low temperatures. *Surf. Coat. Technol.* **1999**, *116–119*, 205–211. [CrossRef]
47. Gontijo, L.C.; Machado, R.; Casteletti, L.C.; Kuri, S.E.; Nascente, P.A.P. X-ray diffraction characterisation of expanded austenite and ferrite in plasma nitrided stainless steels. *Surf. Eng.* **2010**, *26*, 265–270. [CrossRef]
48. Panicaud, B.; Chemkhi, M.; Roos, A.; Retraint, D. Theoretical modelling of iron nitriding coupled with a nanocrystallisation treatment. Application to numerical predictions for ferritic stainless steels. *Appl. Surf. Sci.* **2012**, *258*, 6611–6620. [CrossRef]
49. Pinedo, C.E.; Varela, L.B.; Tschiptschin, A.P. Low-temperature plasma nitriding of AISI F51 duplex stainless steel. *Surf. Coat. Technol.* **2013**, *232*, 839–843. [CrossRef]
50. Alphonsa, J.; Raja, V.S.; Mukherjee, S. Study of plasma nitriding and nitrocarburizing for higher corrosion resistance and hardness of 2205 duplex stainless steel. *Corros. Sci.* **2015**, *100*, 121–132. [CrossRef]
51. Maleque, M.A.; Lailatul, P.H.; Fathaen, A.A.; Norinsan, K.; Haider, J. Nitride alloy layer formation of duplex stainless steel using nitriding process. *IOP Conf. Ser. Mater. Sci. Eng.* **2018**, *290*, 012015. [CrossRef]
52. Blawert, C.; Weisheit, A.; Mordike, B.L.; Knoop, R.M. Plasma immersion ion implantation of stainless steel: Austenitic stainless steel in comparison to austenitic-ferritic stainless steel. *Surf. Coat. Technol.* **1996**, *85*, 15–27. [CrossRef]
53. Chiu, L.H.; Su, Y.Y.; Chen, F.S.; Chang, H. Microstructure and Properties of Active Screen Plasma Nitrided Duplex Stainless Steel. *Mater. Manuf. Process.* **2010**, *25*, 316–323. [CrossRef]
54. Tschiptschin, A.P.; Varela, L.B.; Pinedo, C.E.; Li, X.Y.; Dong, H. Development and microstructure characterization of single and duplex nitriding of UNS S31803 duplex stainless steel. *Surf. Coat. Technol.* **2017**, *327*, 83–92. [CrossRef]
55. Li, X.; Dou, W.; Tian, L. Combating the Tribo-Corrosion of LDX2404 Lean Duplex Stainless Steel by Low Temperature. *Lubricants* **2018**, *6*, 93. [CrossRef]
56. Mesa, D.H.; Pinedo, C.E.; Tschiptschin, A.P. Improvement of the cavitation erosion resistance of UNS S31803 stainless steel by duplex treatment. *Surf. Coat. Technol.* **2010**, *205*, 1552–1556. [CrossRef]
57. Bobadilla, M.; Tschiptschin, A. On the Nitrogen Diffusion in a Duplex Stainless Steel. *Mater. Res.* **2015**, *18*, 390–394. [CrossRef]

58. Llorca-Isern, N.; López-Luque, H.; López-Jiménez, I.; Biezma, M.V. Identification of sigma and chi phases in duplex stainless steels. *Mater. Charact.* **2016**, *112*, 20–29. [CrossRef]
59. Llorca-Isern, N.; Biserova-Tahchieva, A.; Lopez-Jimenez, I.; Calliari, I.; Cabrera, J.M.; Roca, A. Influence of severe plastic deformation in phase transformation of superduplex stainless steels. *J. Mater. Sci.* **2019**, *54*, 2648–2657. [CrossRef]